Desalination and Water Treatment
www.deswater.com

doi: 10.5004/dwt.2022.28523

260 (2022) 179–186
June

Fe_3O_4/MMT Fenton-like heterogeneous catalyst for the methylene blue degradation

Hassan Ayadi[a,d,*], Ammar Khaled[b], Sabrina Halladja[c], Issam Boudraa[d], Zehoua Rehimi[a], Mohamed M. Chehimi[e]

[a]*Laboratory of Physico-Chemistry Research of Surfaces and Interfaces, Faculty of Sciences, University of 20 Août 1955, Skikda 21000, Algeria, emails: ayahadz@yahoo.fr (H. Ayadi), zehoua.rehimi@gmail.com (Z. Rehimi)*
[b]*Department of Chemistry, Faculty of Exact Sciences and Informatics, Mohamed Seddik Benyahia University, Jijel-18000, Algeria, email: ammark90@gmail.com*
[c]*Laboratory of Anticorrosion-Materials, Environment and Structures, Faculty of Sciences, University of 20 Août 1955, Skikda 21000, Algeria, email: sabrinahalladja@gmail.com*
[d]*Research Unit of Environmental Chemistry, and Structural Molecular, Constantine1 University, 25000 Constantine, Algeria, email: issam.boudraa@gmail.com*
[e]*University Paris Est Creteil, CNRS, ICMPE, UMR7182, F-94320 Thiais, France, email: mmchehimi@yahoo.fr*

Received 11 December 2021; Accepted 17 April 2022

ABSTRACT

Modified clay materials constitute a unique series of materials for effective and efficient heterogeneous catalytic oxidation applied to environmental remediation. In this work, magnetite-decorated montmorillonite catalyst (Fe_3O_4/MMT) was prepared by co-precipitation method and then characterized by Fourier-transform infrared spectroscopy, X-ray diffraction, X-ray photoelectron spectroscopy, scanning electron microscopy and UV-visible spectroscopy. Montmorillonite show interesting properties in adsorption and catalysis. Moreover the Fe_3O_4 nanoparticles mainly existed on the surface of the MMT, thus exhibiting improved dispersion and lower levels of aggregation. The catalytic activity of Fe_3O_4/MMT was interrogated in advanced oxidation process using methylene blue (MB) as a model pollutant. The catalyzed degradation of MB was conducted in the presence of H_2O_2. Fe_3O_4/MMT showed a higher degradation efficiency compared to MMT and Fe_3O_4. This survey was optimized by a change in initial H_2O_2 concentration and temperature; the results obtained show a quasi-complete removal of the MB color. This study confirmed the catalytic efficiency of Fe_3O_4/MMT material for MB removal by heterogeneous Fenton oxidation. In addition, the synthesized material was easily recovered by simple magnetic separation which accounts for good reusability and remarkable catalytic stability.

Keywords: Heterogeneous Fenton catalysts; Methylene blue; Fe_3O_4; Montmorillonite decolonization ratio

1. Introduction

Tackling water pollution is an important issue that requires strict control at the global level. Various chemicals that exist in nature or released from anthropogenic activities are the main resources of water pollution. Residual effluents of industry often contain a variety of contaminants. Organic dyes are one of the pollutants that threaten the environment. Each year, more than 700,000 tonnes of dyes are produced worldwide while about 12% of the dyes are directly released into waters compartment [1].

* Corresponding author.

They are characterized by their complex structures and higher molecular weights, which make them recalcitrant and persistent in the environment [2–5]. Numerous types of dyes are toxic, carcinogenic and mutagenic to a broad selection of living species [6,7].

The various water treatment and purification technologies have been widely discussed in literature, but the design and operation of the methods remains a challenge to date. It should be stressed here that every method has its own technical or economic limits for tangible applications [8,9].

Recent developments in the chemical water treatment field have led to an improvement in oxidative degradation processes of organic compounds in aqueous media; this is through the application of catalytic and photochemical methods. In the course of the last twenty years, new treatment processes have emerged including advanced oxidation processes (AOPs), which have proven to be very useful for the treatment of high-organic loading and non-biodegradable in the wastewater [10,11].

Fenton's reagent is commonly used in AOPs process because it has several advantages such as high efficiency of oxidation, mild reaction conditions, environmentally friendly materials and simple operation [12,13]. H_2O_2/Fe^{2+} mixtures have very powerful oxidizing properties in an acidic medium due to the generation of hydroxyl radicals (HO·). These radical species are well known to be very efficient and non-selective in the degradation of persistent organic pollutants. The production of hydroxyl radicals can be explained by the following equations [14,15].

$$Fe^{2+}_{(aq)} + H_2O_2 \rightarrow Fe^{3+}_{(aq)} + HO^{\bullet} + HO^{-} \quad k_1 = 76\ M^{-1}\cdot s^{-1} \tag{1}$$

$$HO^{\bullet} + Fe^{2+}_{(aq)} \rightarrow Fe^{3+}_{(aq)} + HO^{-} \quad k_2 = 3\times 10^{8}\ M^{-1}\cdot s^{-1} \tag{2}$$

Under acidic environments where pH is between 2.7 and 2.8, Fe^{3+} is reduced to Fe^{2+}:

$$Fe^{3+}_{(aq)} + H_2O_2 \rightleftharpoons FeOOH^{2+} + H^{+} \quad k_3 = 3.1\times 10^{-3}\ M^{-1}\cdot s^{-1} \tag{3}$$

$$FeOOH^{2+} \rightarrow HO^{\bullet}_2 + Fe^{2+}_{(aq)} \quad k_4 = 2.7\times 10^{-2}\ M^{-1}\cdot s^{-1} \tag{4}$$

and $HO^{\bullet}_2$ regenerated $Fe^{2+}_{(aq)}$

$$HO^{\bullet}_2 + Fe^{2+}_{(aq)} \rightarrow HO^{-}_2 + Fe^{3+}_{(aq)} \tag{5}$$

$$Fe^{3+}_{(aq)} + HO^{\bullet}_2 \rightarrow Fe^{2+}_{(aq)} + O_2 + H^{+} \quad k_5 < 2\times 10^{3}\ M^{-1}\cdot s^{-1} \tag{6}$$

However, homogenous Fenton process presents some disadvantages such as the formation of large amount of ferrous iron sludge which causes secondary pollution problems, and the control of pH becomes difficult, within very strict range, for a good progress of the reaction [16–18].

Some heterogeneous catalysts with low iron dissolution, such as nanoparticulate zero-valent iron, iron oxides and immobilized iron on clays have replaced Fe^{2+}/Fe^{3+} solutions to avoid accumulation and precipitation of soluble iron [19].

Heterogeneous Fenton oxidation has proven to be an efficient and economical method, where iron is immobilized on solid supports such as clays and carbon nanotubes [20]. In the presence of a suitable oxidant, these composite materials can remove organic contaminants over a wide pH range and reduce the loss of iron catalyst.

Particular attention has been given to magnetite, Fe_3O_4, in the treatment of recalcitrant organic compounds for two reasons; on the one hand for its excellent chemical stability and on the other hand the formation of reactive $HO^{\bullet}$ radicals when it is coupled to H_2O_2.

The combination of clays such as montmorillonite with magnetite nanoparticles and a appropriate oxidant provides a new composite material exhibiting synergic behavior or complementary to the constituents. This can be explained by the fact that montmorillonite has interesting properties in adsorption and catalysis, while Fe_3O_4 contains on the one hand Fe^{2+} and Fe^{3+} cations, which are crucial in the initiation of the Fenton reaction, and on the other hand, has great advantages for the aforementioned applications [21,22].

Indeed, magnetite-based catalysts are easily recovered and reused for several cycles in the heterogeneous Fenton process. The dissolution of iron ions in the aqueous phase is very limited or even insignificant; a very small quantity of iron ions is released from the catalyst during the degradation of organic pollutants. At this stage hydrogen peroxide oxidizes ferrous ions to produce hydroxyl radicals rapidly, leading to a rapid decrease in ferrous ions in solution [23].

In this work, we synthesized a nanocomposite Fe_3O_4/MMT for Fenton-like decoloration an azo dye which is methylene blue (MB). It is used in several sectors such as chemistry, pharmacology, medicine, biology and textiles. The use of this dye presents a potential risk to the environment and human health. This is why, it is imperative to be concerned about the impact of these substances on this environmental compartment.

The catalyst Fe_3O_4/MMT was prepared using the co-precipitation method. The Fenton-like catalytic performance of this catalyst to decolorize MB was been evaluated. Similar studies has been conducted on degradation of some persistent pollutants such as antibiocs (Ofloxacin) and pesticides (phenol) [24].

Features mentioned previously made us excited for the synthesis and characterization of a composite material based on magnetite and montmorillonite by co-precipitation route. The elaborated composite was evaluated in the removal of methylene blue by the heterogeneous Fenton-like process.

2. Experimental

2.1. Materials

Anhydrous ferric sulfate ($Fe_2(SO_4)_3$), ferrous sulfate ($FeSO_4{\cdot}7H_2O$) and hydrogen peroxide (H_2O_2, 25% wt.) were

purchased from BIOCHEM. Montmorillonite K10, was purchased from Sigma-Aldrich (Germany).

Methylene blue (cationic dye) taken as a pollutant model was used without any prior purification. The solutions were prepared by dissolving the amounts of the dye in distilled water.

2.2. Preparation of the modified montmorillonite

Magnetite/montmorillonite (Fe_3O_4/MMT) composite was synthesized by co-precipitation method [25]. Initially, in a three-necked round-bottomed flask (500 mL), the MMT (4.0 g) was dispersed into 200 mL of an aqueous solution in which $Fe_2(SO_4)_3$ (4.9 g, 12.25 mmol) was dissolved. The mixture was stirred for 12 h in order to obtain a stable suspension. Once the 12 h of stirring reached, $FeSO_4{\cdot}7H_2O$ (1.72 g 6.18 mmol) was added in the flask under N_2 atmosphere. This solution was heated till 90°C and then NH_4OH (6.0 mL, 25%, wt./wt.) was added rapidly. A black precipitate appeared immediately and the mixture was kept under stirring for another hour. After cooling to room temperature, the precipitate of modified montmorillonite was separated by centrifugation and washed successively with distilled water. The obtained product was finally dried at 80°C and has been ready for use. For comparison study, pure Fe_3O_4 NPs were also prepared via an analogous method but in the absence of any MMT. The relevant chemical reaction can be expressed as follows:

$$2Fe^{3+} + Fe^{2+} + 8OH^- + MMT \rightarrow MMT - Fe_3O_4 + 4H_2O \quad (7)$$

2.3. Characterization methods

The montmorillonite and its magnetic composite were characterized by X-ray diffraction (XRD) using an X'pert-PRO panalytical powder diffractometer. The data recording were carried out within an angle range from 20° to 80° with a step of 0.013° using a 0.154056 nm wavelength radiation of copper anode (CuKα radiation, 45 kV, 40 mA). The diffraction data were analyzed with a PanalyticalX' Pert High Score Plus software. The crystalline phases were determined compared to registered models of the PDF3 database. The morphology of the composite was observed using a scanning electron microscope JEOL JCM-5000 Neoscope scanning electron microscopy (SEM). Fourier-transform infrared (FTIR) spectra were recorded between 400 and 4,000 cm^{-1} using a spectrometer Thermo Scientific Model Nicolet IS10 equipped with an ATR measuring device (Attenuated Total Reflexion) Golden Gate Model, with a Specac Model Diamond Crystal.

X-ray photoelectron (XPS) spectra were recorded using a Thermo Fisher K-Alpha spectrometer using a monochromatic AlKαX-ray beam (1486.6 eV, 300 μm spot size). The samples were outgassed before they were introduced into the analysis chamber at about 2×10^{-8} Pa. Pass energy was 200 eV for survey and 20 eV for high-resolution spectra. The Thermo Scientific Advantage Software (version 5.943) was used for collecting and processing the spectra. The binding energy shifts were calibrated relative to the adventitious carbon C1s position fixed at 284.6 eV and the BE accuracy was ±0.1 eV.

3. Results and discussion

3.1. Infrared spectroscopic characterizations

The Fourier-transform infrared spectra of montmorillonite and modified composite are shown in Fig. 1. The absorption band at about 3,404 cm^{-1} can be attributed to the water molecule vibration [26]. Furthermore, the three absorption bands located at 1,040, 792 and 526 cm^{-1} are the characteristic peaks of Si–O stretching vibrations. As can be observed, the intensity of the Si–O bands in the Fe_3O_4/MMT composite is lower than that of MMT, indicating an interaction between Fe–O and Si–O bands on the surface of Fe_3O_4/MMT [25,27]. This means that Fe–O was probably bound to the surface of MMT during the synthesis procedure.

3.2. XRD analysis

XRD analysis of MMT and Fe_3O_4/MMT are shown in Fig. 2. The patterns confirm the presence of magnetite in the obtained composite, with the appearance of new characteristic peaks of magnetite at 2θ = 30.09°, 35.64° and 62.94°

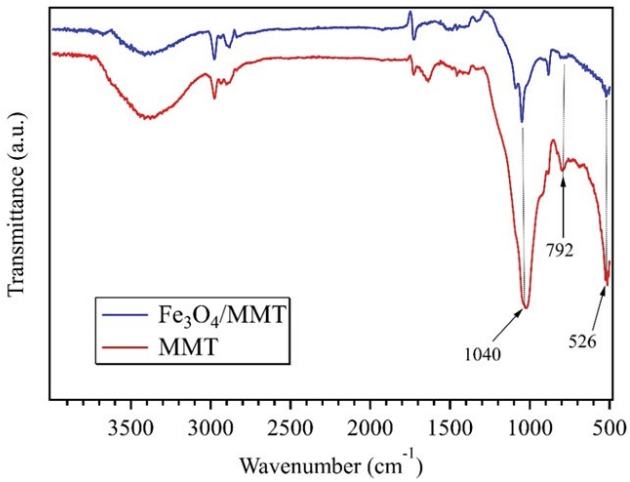

Fig. 1. FTIR spectra of MMT and Fe_3O_4/MMT.

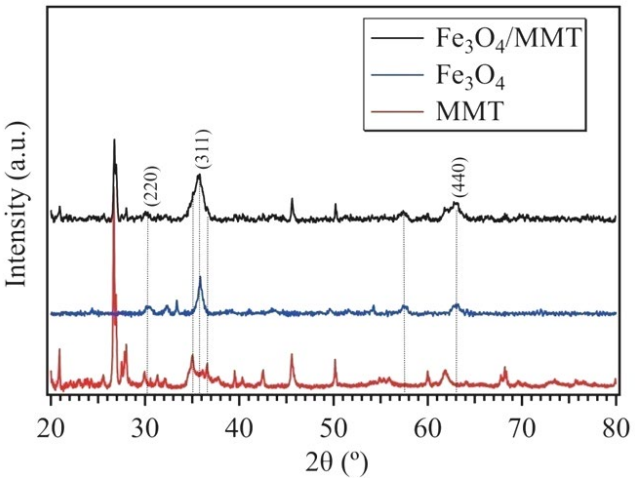

Fig. 2. X-ray diffraction pattern of MMT, Fe_3O_4 and Fe_3O_4/MMT.

corresponding to (220), (311) and (440) reflections, respectively (ICDD-PDF No 00-019-0629). The other diffraction peaks at 2θ = 26.73°, 29.99°, 35.07°, 54.23°, 40.37°and 61.93° are clearly attributed to MMT (ICDD-PDF No 00-029-1498).

3.3. XPS analysis

Survey spectra are displayed in Fig. 3 with Al2p, Si2p, O1s and Fe2p major peak assignments; C1s is due to unavoidable hydrocarbon contamination.

High-resolution spectra are used to verify the chemical nature of the elements present at the surface of MMT and Fe_3O_4/MMT composite, particularly O1s and Fe2p. As shown in Fig. 4a, the O1s peak is fitted with four components centered at 529.4, 531.0, 532.0 and 534.1 eV assigned to Fe_3O_4, possibly hydroxides, Al–O–Si and organic contamination. The Fe2p region (Fig. 4b) exhibits spin-orbit coupling which resulted in $Fe2p_{3/2}$ and $2p_{1/2}$ peaks located at 710.8 and 724.4 eV respectively, which account for Fe_3O_4 oxide [28–30].

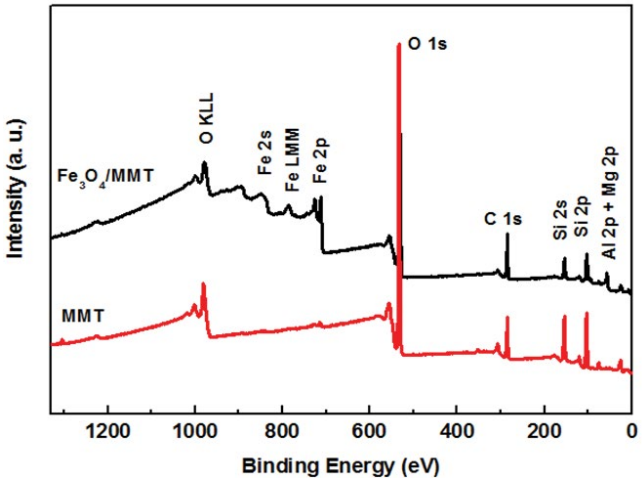

Fig. 3. XPS survey of MMT and Fe_3O_4/MMT composite.

3.4. SEM analysis

The MMT and Fe_3O_4/MMT micrographs (Fig. 5) obtained by scanning electron microscopy (SEM) shows clear and visible contrast in the morphology between MMT and Fe_3O_4/MMT. The MMT surface has an aggregated morphology with an irregular plate like shape (Fig. 5a). After the modification of MMT with magnetite, the particle size is slightly reduced as seen in Fig. 5b.

3.5. Magnetic properties

The magnetic properties of the Fe_3O_4/MMT composite were studied by vibrating sample magnetometry (VSM) at 298 K. Fig. 6, shows the magnetic hysteresis loop of Fe_3O_4/MMT. It can be seen that the values of magnetization (Ms) are 35 emu/g, compared to the theoretical Ms value of magnetite [31] which is generally 92 to 100 emu/g, the Ms of the composite is relatively low. This may be due to the introduction of the non-magnetic MMT particles. However the saturation magnetization of as-prepared composite material is sufficient to meet the needs of magnetic separation. In the presence of an external magnetic field, the catalyst was attracted to the wall of the flask in a short time compared to a homogeneous dispersion without an extrinsic magnetic magnet (Inset of Fig. 6).

3.6. Catalytic performances of Fe_3O_4/MMT in the catalyzed MB degradation

The catalytic performances of Fe_3O_4/MMT were evaluated through the heterogeneous Fenton degradation of MB under the assistance of H_2O_2 (MB: 50 mg/L, catalysts: 0.5 g/L, pH: 3.0, H_2O_2: 6.65 g/L, *T*: 20°C). Batch experiments were performed in order to investigate the removal efficiency of MB dye. All the reactions were carried out in the darkness to avoid the effect of light onto the degradation. The results obtained are shown in Fig. 7.

Fig. 7 clearly shows that discoloration of MB is negligible with H_2O_2 only (Fig. 7a). Nearly 15% of MB was removed

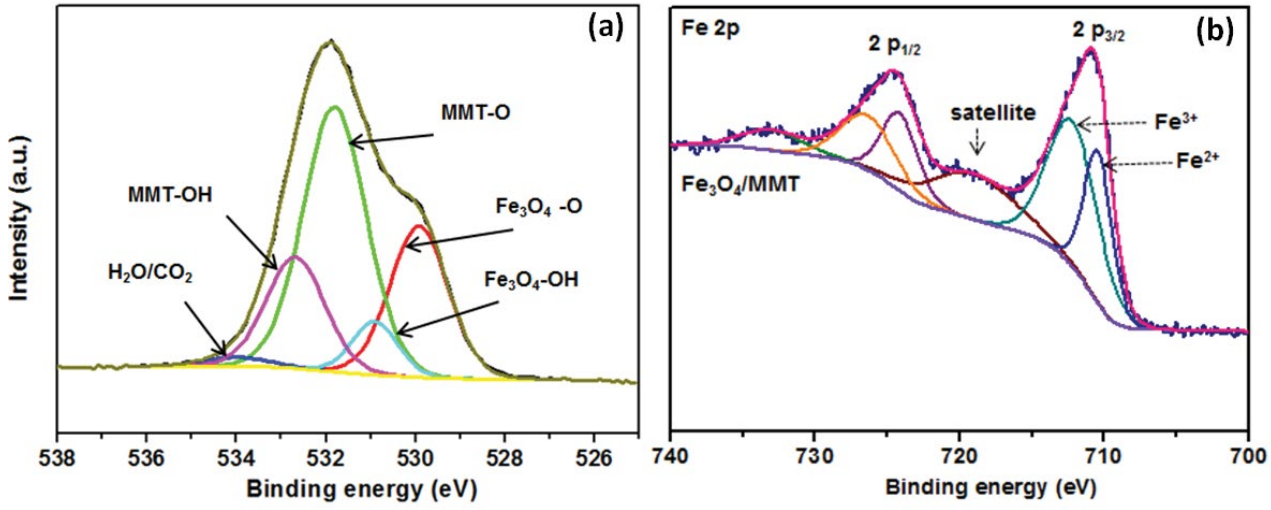

Fig. 4. High-resolution spectrum of O1s (a) and Fe2p (b) from MMT and Fe_3O_4/MMT.

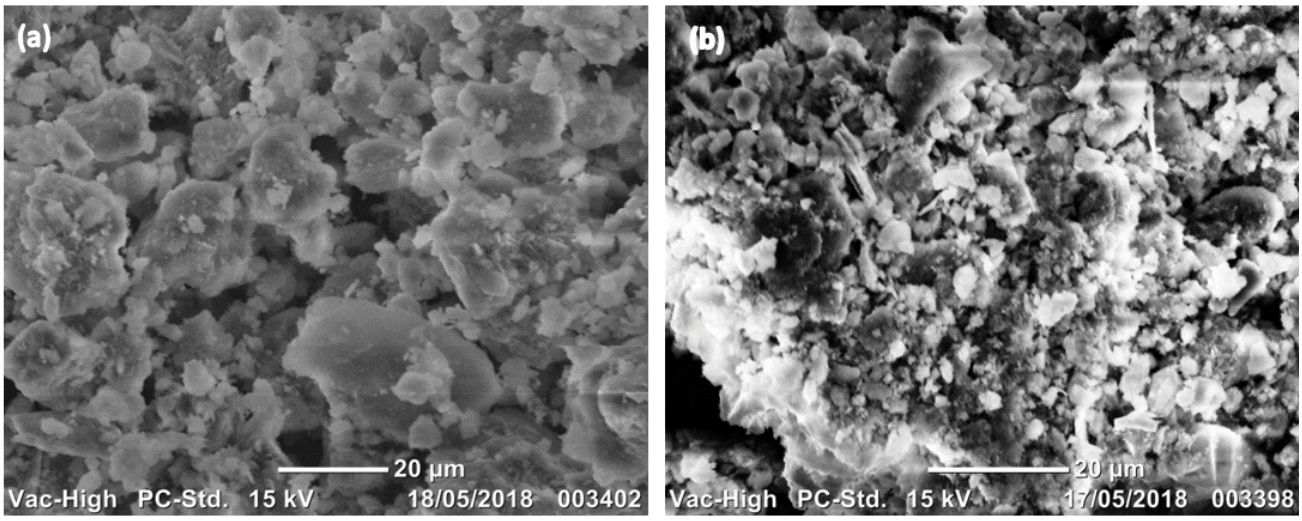

Fig. 5. SEM images of MMT (a) and Fe_3O_4/MMT (b).

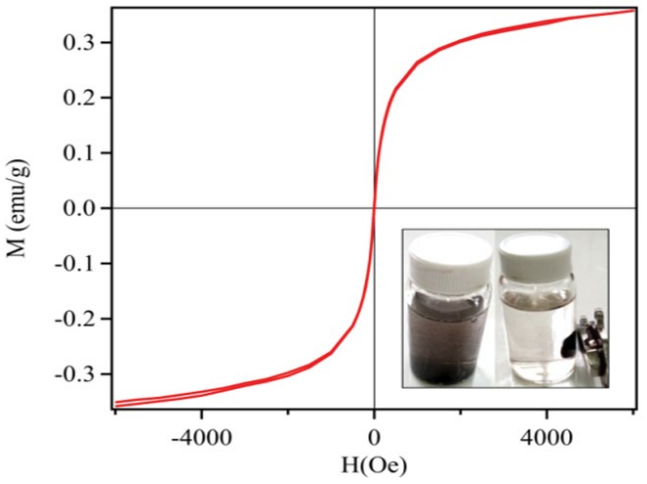

Fig. 6. Magnetic hysteresis curve of Fe_3O_4/MMT. The inset pattern is a photograph of magnetic separation of the Fe_3O_4/MMT from solution.

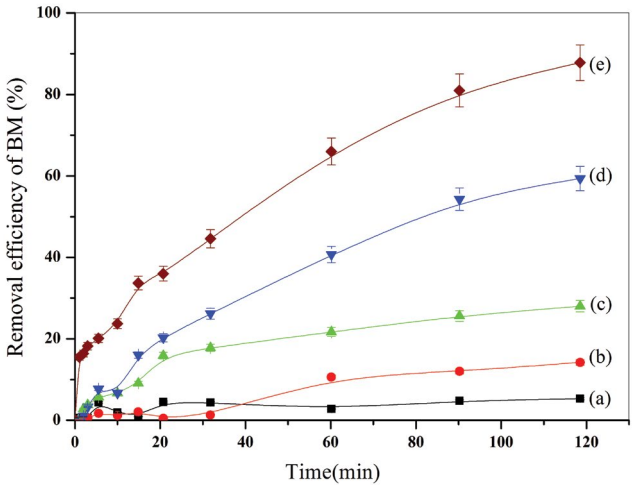

Fig. 7. MB removal with various catalysts: H_2O_2 (a), Fe_3O_4 (b), Fe_3O_4 + H_2O_2 (c), Fe_3O_4/MMT (d) and Fe_3O_4/MMT + H_2O_2 (e); MB = 50 mg/L; [H_2O_2] = 6.65 g/L; pH = 3; T = 20°C; catalyst = 0.5 g/L.

in 120 min in the presence of Fe_3O_4 (Fig. 7b). The combination of Fe_3O_4 with H_2O_2 returned better results, yet levelling off at 22% removal of MB within 120 min. In contrast, the removal efficiency of MB increased to 60% in the presence of Fe_3O_4/MMT (Fig. 7d) and jumped to 90% when the catalyzed reaction was conducted in the presence of both Fe_3O_4/MMT and H_2O_2 (Fig. 7e).

These results indicated that the higher removal efficiency of MB dye from aqueous medium is obtained with Fe_3O_4/MMT catalyst in the presence of H_2O_2.

This can be explained by the production of the hydroxyl radicals from the reaction of H_2O_2 with the iron oxide immobilized on the surface of the composite. The dye removal efficiency by this catalyst is probably due to a synergy effect of adsorbed peroxide and Fe_3O_4/MMT composite, which improves the degradation of the organic compounds. Indeed, previous studies show that the presence of iron oxide, Fe(II) and Fe(III), immobilized on the composite surface promotes the adsorption of H_2O_2 and the conversion of H_2O_2 to $OH^{\bullet}$ radicals [32].

3.7. Optimization of H_2O_2 concentration

The concentration of hydrogen peroxide plays an important role in the effectiveness of Fenton oxidation on the degradation of methylene blue.

The reaction rate constants are described by Eq. (8),

$$-\left[\mathrm{MB}\right]_t = k_{\mathrm{app}} \cdot t - \left[\mathrm{MB}\right]_0 \tag{8}$$

where $[MB]_t$: is the concentration of the methylene blue at time t, $[MB]_0$ is the initial concentration of the dye at time t = 0, and k_{app} is the apparent rate constant of the methylene blue degradation reaction. The calculated apparent

rate constants and the coefficients of determination R^2 are reported in Table 1.

The results reported in Table 1 clearly show that the degradation of MB is effective with a hydrogen peroxide concentration equal to 6.65 g/L. In this case the calculated rate constant k_{app} is equal to 1.60×10^{-2} min^{-1} and the determination coefficient R^2 is very close to 1. An increase in the concentration of H_2O_2 improves the rate of MB discoloration. However we have noted that a higher concentration of H_2O_2 on the order of 8.46 g/L implies a decrease in the rate of discoloration of MB (29.1×10^{-3}). This is due to the excess of H_2O_2 which favours the recombination between the hydroxyl radicals on the one hand and the reaction between the hydroxyl radicals and hydrogen peroxide on the other hand according to the following reactions (9) and (10):

$$OH^{\bullet} + OH^{\bullet} \rightarrow H_2O_2 \quad (9)$$

$$OH^{\bullet} + H_2O_2 \rightarrow H_2O + HO_2^{\bullet} \quad (10)$$

3.8. Influence of temperature on MB removal efficiency

MB removal was investigated in the temperature range of 10°C–60°C with 10°C increments. The tests were carried out by adding 50 mg of Fe_3O_4/MMT composite to 100 mL of MB solution with concentration of 50 mg/L at pH = 3 and in the presence of H_2O_2 at 6.65 g/L.

As noted from Fig. 8, the rate of MB degradation is notably improved with increasing reaction temperature. It was observed that the color removal rate of MB was quasi-total at T = 50°C. The increase of the temperature shortened the time of the reaction where about 99.5% of MB is eliminated after 30 min.

The initial removal rate at 50°C is higher than that observed at 60°C, this can be explained by the fact that when temperatures increase, it leads to the thermal decomposition of hydrogen peroxide into O_2 and H_2O, which prevents the formation of hydroxyl radicals and reduce the removal rate of dye [23,33].

From the calculated values of reaction rate (Table 2), an increase was observed when the temperature raised.

This can be explained by the fact that between 10°C and 50°C the heterogeneous Fenton process is endothermic reaction [34]. Besides, an increase in temperature could also facilitate the activation of the hydrogen peroxide and the diffusion of the reagents to the surface of the catalyst. The determined activation energy was 38.50 kJ/mol for Fe_3O_4/MMT/H_2O_2. This value indicated that the degradation of MB by Fe_3O_4/MMT/H_2O_2 catalyst through heterogeneous Fenton reaction in temperature range between 20°C and 50°C did not require a very high energy [35].

Table 3 shows the comparison of k_{app} values of MB degradation obtained in our study with those described in the literature for other types of catalytic nanocomposites. We observed that the value of apparent rate constant calculated under optimum conditions is 11.0×10^{-2} min^{-1} which is higher than reported in the literature.

3.9. Catalytic stability of the Fe_3O_4/MMT

The reusability of a heterogeneous catalyst is crucial for its practical application and the resilience of a catalyst to reaction conditions is often expressed by its ability to be reused. For this purpose and to evaluate the

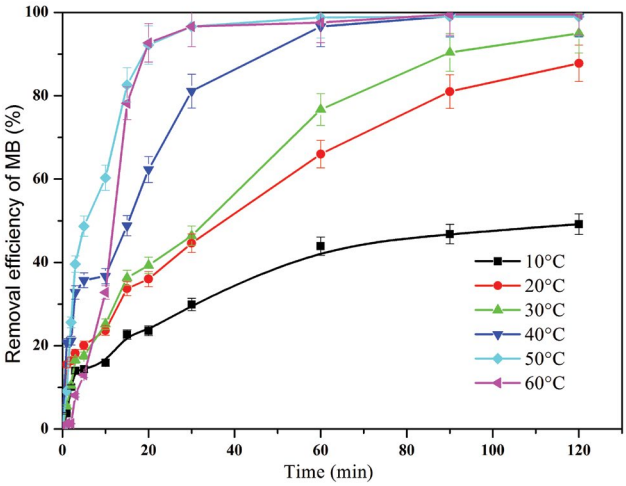

Fig. 8. Influence of temperature on MB removal efficiency. [MB] = 50 mg/L; pH = 3; [H_2O_2] = 6.65 g/L; catalyst = 0.5 g/L.

Table 1
Values of apparent rate constants and the coefficients of determination of methylene blue degradation at different concentration of H_2O_2

[H_2O_2] (g/L)	0	1.66	3.32	4.99	6.65	8.32
k_{app} (min^{-1})	8.82×10^{-3}	1.26×10^{-2}	1.29×10^{-2}	1.32×10^{-2}	1.60×10^{-2}	2.95×10^{-3}
R^2	0.994	0.989	0.988	0.959	0.986	0.958

Table 2
Values of apparent rate constants and the coefficients of determination of methylene blue degradation

T (°C)	10	20	30	40	50	60
k_{app} (min^{-1})	8.7×10^{-3}	1.61×10^{-2}	2.27×10^{-2}	5.35×10^{-2}	11.0×10^{-2}	7.60×10^{-2}
R^2	0.940	0.975	0.984	0.982	0.986	0.830

Table 3
Comparison of rate constant of degradation of MB dye over different kinds of nanocomposites

Nanocomposite	Conditions	Mass catalyst/Volume (g/L)	k_{app} (min^{-1})	R^2	Reference
Mesoporous silica magnetite (MCM-MAG)	H_2O_2: 0.097 M; MB: 50 mg/L; 25°C	0.1	1.8×10^{-3}	0.92	[33]
Magnetic porous carbon microspheres (MPCMS-500)	H_2O_2: 16 mM; NH_2OH: 4 mM; MB: 40 mg/L; pH 5; 30°C	2	10.5×10^{-2}	0.998	[34]
Graphene oxide supported magnetite (Mt-GO)	H_2O_2: 2.05 mM; MB: 10 mg/L: pH 3.0; 25°C	0.013	7.5×10^{-3}	0.98	[35]
Titanomagnetite	H_2O_2: 0.30 M; MB: 100 mg/L; 30°C; pH 6.8	1.0	2.15×10^{-3}	0.994	[36]
	H_2O_2: 0.30 M; MB: 100 mg/L; 50°C; pH 6.8	1.0	8.52×10^{-3}	0.999	
Fe_3O_4/MMT	H_2O_2: 6.65 g/L (0.19 M); MB: 50 mg/L; 20°C; pH 3.0	0.5	1.60×10^{-2}	0.975	This study
	H_2O_2: 6.65 g/L (0.19 M); MB: 50 mg/L; 30°C; pH 3.0	0.5	2.27×10^{-2}	0.984	
	H_2O_2: 6.65 g/L (0.19 M); MB: 50 mg/L; 50°C; pH 3.0	0.5	11.0×10^{-2}	0.986	

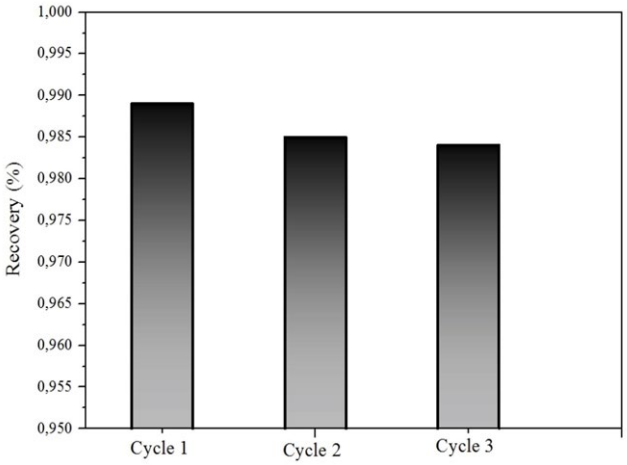

Fig. 9. Reuse of Fe_3O_4/MMT. Reaction conditions: MB = 50 mg/L; H_2O_2 = 6.65 g/L; catalyst = 50 mg/L; T = 50°C; pH = 3.

catalytic stability of the Fe_3O_4/MMT catalyst in the oxidation medium of H_2O_2, the particles were repeatedly recovered to perform successive MB degradation tests. The evaluation of the capacity and the stability of the composite via the Fenton reaction were tested for three successive cycles (Fig. 9). MB discoloration efficiency was around 99% after the third use.

4. Conclusion

In this study, the composite material Fe_3O_4/MMT was prepared and used as a catalyst for the degradation of methylene blue in a heterogeneous Fenton-like process. XRD, FTIR, SEM and XPS characterization results confirmed the presence of magnetite in the modified montmorillonite. Optimal reaction conditions for the degradation of MB were found to be an initial pH of 3, an initial H_2O_2 concentration of 6.65 g/L and a reaction temperature of 50°C. Under these conditions the rate of discoloration of the MB solution is almost total (about 99%), which confirms the catalytic effect of the material developed. This removal efficiency by this catalyst is probably due to the effective contribution of the adsorbed peroxide on to Fe_3O_4/MMT composite, which improves the degradation of organic compounds.

It should also be noted that this process allows easy recovery of the catalyst due to the magnetic properties of the composite.

The tests of the reusability of the composite showed a catalytic behavior which could be reproduced in consecutives experiments without significant drop recovery.

Acknowledgements

The authors are indebted to the University 20 Août 1955 for financial support. The authors thank Pr. Brahim Kebabi (Pollution and Water Treatment Laboratory, Constantine 1 University) and Dr. Debbah Younes for their technical supports.

References

[1] L. Zhang, H. Zhang, Y. Tian, Z. Chen, L. Han, Adsorption of methylene blue from aqueous solutions onto sintering process red mud, Desal. Water Treat., 47 (2012) 31–41.
[2] B.E. Barragán, C. Costa, M. Carmen Márquez, Biodegradation of azo dyes by bacteria inoculated on solid media, Dyes Pigm., 75 (2007) 73–81.
[3] R. Jain, V.K. Gupta, S. Sikarwar, Adsorption and desorption studies on hazardous dye Naphthol Yellow S, J. Hazard. Mater., 182 (2010) 749–756.
[4] V. Hernández-Montoya, M.A. Pérez-Cruz, D.I. Mendoza-Castillo, M.R. Moreno-Virgen, A. Bonilla-Petriciolet, Competitive adsorption of dyes and heavy metals on zeolitic structures, J. Environ. Eng. Manage., 116 (2013) 213–221.
[5] Z. Rehimi, H. Ayadi, S. Halladja, Synthesis and characterization of Fe_3O_4–MWCNTs adsorbent: application for bromocresol

purple dye removal in aqueous medium, J. New Technol. Mater., 10 (2020) 31–37.
[6] S. Shojaei, S. Khammarnia, S. Shojaei, M. Sasani, Removal of Reactive Red 198 by nanoparticle zero valent iron in the presence of hydrogen peroxide, J. Water Environ. Nanotechnol., 2 (2017) 129–135.
[7] M. Kaykhaii, M. Sasani, S. Marghzari, Removal of dyes from the environment by adsorption process, Chem. Mater. Eng., 6 (2018) 31–35.
[8] A. Bonilla-Petriciolet, D.I. Mendoza-Castillo, H.E. Reynel-Ávila, Adsorption Processes for Water Treatment and Purification, Springer International Publishing, Cham, Switzerland, 2017.
[9] I. Boudraa, S.U. Odabasi, H. Ayadi, B. Kebabi, Preparation, Characterization and Adsorption Capacity of Zn(II) and Cu(II) of Natural Bentonite Modified with Magnetite, Proceeding of 5th International Conference on Engineering Sciences, Ankara-Turkey, 2019, pp. 286–291.
[10] Y. Wang, H. Zhao, J. Gao, G. Zhao, Y. Zhang, Y. Zhang, Rapid mineralization of azo-dye wastewater by microwave synergistic electro-Fenton oxidation process, J. Phys. Chem. C, 116 (2012) 7457–7463.
[11] N.N. Tušar, D. Maučec, M. Rangus, I. Arčon, M. Mazaj, M. Cotman, A. Pintar, V. Kaučič, Manganese functionalized silicate nanoparticles as a Fenton-type catalyst for water purification by advanced oxidation processes (AOP), Adv. Funct. Mater., 22 (2012) 820–826.
[12] T. Zhang, H. Zhu, J.-P. Croué, Production of sulfate radical from peroxymonosulfate induced by a magnetically separable $CuFe_2O_4$ spinel in water: efficiency, stability, and mechanism, Environ. Sci. Technol., 47 (2013) 2784–2791.
[13] Y. Yao, Y. Cai, F. Lu, F. Wei, X. Wang, S. Wang, Magnetic recoverable $MnFe_2O_4$ and $MnFe_2O_4$-graphene hybrid as heterogeneous catalysts of peroxymonosulfate activation for efficient degradation of aqueous organic pollutants, J. Hazard. Mater., 270 (2014) 61–70.
[14] J.J. Pignatello, E. Oliveros, A. MacKay, Advanced oxidation processes for organic contaminant destruction based on the Fenton reaction and related chemistry, Crit. Rev. Env. Sci. Technol., 36 (2006) 1–84.
[15] R. Andreozzi, V. Caprio, A. Insola, R. Marotta, Advanced oxidation processes (AOP) for water purification and recovery, Catal. Today, 53 (1999) 51–59.
[16] B.-H. Moon, Y.-B. Park, K.-H. Park, Fenton oxidation of Orange II by pre-reduction using nanoscale zero-valent iron, Desalination, 268 (2011) 249–252.
[17] E. Hajba-Horváth, E. Biró, M. Mirankó, A. Fodor-Kardos, L. Trif, T. Feczkó, Preparation and in vitro characterization of valsartan-loaded ethyl cellulose and poly(methyl methacrylate) nanoparticles, RSC Adv., 10 (2020) 43915–43926.
[18] L. Liang, L. Cheng, Y. Zhang, Q. Wang, Q. Wu, Y. Xue, X. Meng, Efficiency and mechanisms of rhodamine B degradation in Fenton-like systems based on zero-valent iron, RSC Adv., 10 (2020) 28509–28515.
[19] L. Xu, J. Wang, Magnetic nanoscaled Fe_3O_4/CeO_2 composite as an efficient Fenton-like heterogeneous catalyst for degradation of 4-chlorophenol, Environ. Sci. Technol., 46 (2012) 10145–10153.
[20] N. Dalali, M. Habibizadeh, K. Rostamizadeh, S. Nakisa, Synthesis of magnetite multi-walled carbon nanotubes composite and its application for removal of basic dyes from aqueous solutions, Asia-Pac. J. Chem. Eng., 9 (2014) 552–561.
[21] S.M. Lee, D. Tiwari, Organo and inorgano-organo-modified clays in the remediation of aqueous solutions: an overview, Appl. Clay Sci., 59–60 (2012) 84–102.
[22] N. Belachew, R. Fekadu, A. Ayalew Abebe, RSM-BBD optimization of Fenton-like degradation of 4-nitrophenol using magnetite impregnated kaolin, Air Soil Water Res., 13 (2020) 1–10
[23] S. Kaya, Y. Asci, Application of heterogeneous Fenton processes using Fe(III)/MnO_2 and Fe(III)/SnO_2 catalysts in the treatment of sunflower oil industrial wastewater, Desal. Water Treat., 171 (2019) 302–313.
[24] M. Jin, M. Long, H. Su, Y. Pan, Q. Zhang, J. Wang, B. Zhou, Y. Zhang, Magnetically separable maghemite/montmorillonite composite as an efficient heterogeneous Fenton-like catalyst for phenol degradation, Environ. Sci. Pollut. Res., 24 (2017) 1926–1937.
[25] J. Chang, J. Ma, Q. Ma, D. Zhang, N. Qiao, M. Hu, H. Ma, Adsorption of methylene blue onto Fe_3O_4/activated montmorillonite nanocomposite, Appl. Clay Sci., 119 (2016) 132–140.
[26] L.M. Wu, C.H. Zhou, D.S. Tong, W.H. Yu, H. Wang, Novel hydrothermal carbonization of cellulose catalyzed by montmorillonite to produce kerogen-like hydrochar, Cellulose, 21 (2014) 2845–2857.
[27] M. Hajjaji, H. El Arfaoui, Adsorption of methylene blue and zinc ions on raw and acid-activated bentonite from Morocco, Appl. Clay Sci., 46 (2009) 418–421.
[28] X. Zheng, J. Dou, J. Yuan, W. Qin, X. Hong, A. Ding, Removal of Cs^+ from water and soil by ammonium-pillared montmorillonite/Fe_3O_4 composite, J. Environ. Sci., 56 (2017) 12–24.
[29] B. Zhang, T. Zhang, Z. Zhang, M. Xie, Hydrothermal synthesis of a graphene/magnetite/montmorillonite nanocomposite and its ultrasonically assisted methylene blue adsorption, J. Mater. Sci., 54 (2019) 11037–11055.
[30] G.K. Reddy, P. Boolchand, P.G. Smirniotis, Unexpected behavior of copper in modified ferrites during high temperature WGS reaction—aspects of $Fe^{3+} \leftrightarrow Fe^{2+}$ redox chemistry from Mössbauer and XPS studies, J. Phys. Chem. C, 116 (2012) 11019–11031.
[31] A.S. Teja, P.-Y. Koh, Synthesis, properties, and applications of magnetic iron oxide nanoparticles, Prog. Cryst. Growth Charact. Mater., 55 (2009) 22–45.
[32] H. He, Y. Zhong, X. Liang, W. Tan, J. Zhu, C. Yan Wang, Natural magnetite: an efficient catalyst for the degradation of organic contaminant, Sci. Rep., 5 (2015) 10139, doi: 10.1038/srep10139.
[33] F.C. Ban, X.T. Zheng, H.Y. Zhang, Photo-assisted heterogeneous Fenton-like process for treatment of PNP wastewater, J. Water Sanit. Hyg. Dev., 10 (2020) 136–145.
[34] J. Tang, J. Wang, Fe_3O_4-MWCNT magnetic nanocomposites as efficient Fenton-like catalysts for degradation of sulfamethazine in aqueous solution, ChemistrySelect, 2 (2017) 10727–10735.
[35] J.H. Ramirez, F.J. Maldonado-Hódar, A.F. Pérez-Cadenas, C. Moreno-Castilla, C.A. Costa, L.M. Madeira, Azo-dye Orange II degradation by heterogeneous Fenton-like reaction using carbon-Fe catalysts, Appl. Catal., B, 75 (2007) 312–323.